

NONSTATIONARY EFFECTS IN THE SYSTEM OF COUPLED QUANTUM DOTS INFLUENCED BY COULOMB CORRELATIONS

V. N. Mantsevich^{a,}, N. S. Maslova^a, P. I. Arseev^b*

^a *Lomonosov Moscow State University
119991, Moscow, Russia*

^b *Lebedev Physical Institute, Russian Academy of Sciences
119991, Moscow, Russia*

Received May 6, 2013

We investigate the time evolution of filling numbers of localized electrons in the system of two coupled single-level quantum dots (QDs) connected with the continuous-spectrum states in the presence of Coulomb interaction. We considered correlation functions of all orders for electrons in the QDs by decoupling higher-order correlations between localized and band electrons in the reservoir. We analyze different initial charge configurations and consider Coulomb correlations between localized electrons both within the dots and between the different dots. We reveal the presence of a dynamical charge trapping effect in the first QD in the situation where both dots are occupied at the initial instant. We also find an analytic solution for the time-dependent filling numbers of the localized electrons for a particular configuration of the dots.

DOI: 10.7868/S0044451014010167

1. INTRODUCTION

The control and manipulation of localized charge in small-size systems is one of the most important issues in nanoelectronics [1, 2]. Single semiconductor quantum dots (QDs), which are referred to as “artificial” atoms [3, 4], and coupled QDs — “artificial” molecules [5, 6] — are promising structures to serve for creation of extremely small devices. Several coupled QDs can be used in manufacturing electronic devices dealing with quantum kinetics of individual localized states [7–9]. Therefore, the behavior of coupled QDs in different configurations is currently under careful experimental [10, 11] and theoretical investigation [12, 13].

During the last decade, vertically aligned QDs (for example, indium arsenide QDs in gallium arsenide) have been fabricated and widely studied with great success [14–16]. Such an experimental realization allows organizing a strongly interacting system of QDs with only one of them coupled to the continuous-spectrum states. Consequently, vertically aligned QDs give an opportunity to analyze nonstationary effects in various

charge and spin configurations formation in small-size structures [17].

Lateral QDs seems to be better candidates for controllable electronic coupling between two or several QDs by applying individual lateral gates. That is why they are intensively studied during the last several years both experimentally and theoretically [18, 19].

Investigation of relaxation processes, nonequilibrium charge distribution and nonstationary effects in the electron transport through a system of QDs are vital problems that have to be solved in order to integrate QDs in small quantum circuits [20–26]. Electron transport in such systems is strongly governed by the Coulomb interaction between localized electrons and, of course, by the ratio between the tunneling transfer amplitudes and the QD coupling. Correct interpretation of quantum effects in nanoscale systems gives an opportunity to create high-speed electronic and logic devices [27, 28]. In some of the recent realizations, Coulomb interaction is weak [29], but for small-size QDs, the on-site Coulomb repulsion is in general strong [30], and it is therefore important to take it into account. In some cases, Coulomb correlations can determine time-dependent phenomena [31]. Hence, the problem of time evolution of charge in coupled QDs connected with continuous-spectrum states in the pres-

*E-mail: vmantsev@spmlab.phys.msu.ru

ence of Coulomb correlations between localized electrons is indeed quite topical.

Time evolution of charge states in a semiconductor double quantum well in the presence of Coulomb interaction was experimentally studied in [32]. The authors manipulated the localized charge by the initial pulses and observed pulse-induced tunneling electron oscillations. Localized charge relaxation in the single and coupled quantum wells in the absence of Coulomb interaction was theoretically analyzed by Gurvitz [33, 34]. The author took only two time scales governing the charge time evolution into account and neglected the third time scale that is responsible for charge redistribution between different wells. Time dependence of the accumulated charge and the tunneling current through a single QD in the presence of Coulomb interaction were theoretically analyzed in [35]. The authors described relaxation processes and revealed three time rates for localized charge relaxation in the QD coupled to a thermostat. Several different time rates were also found in the system of two and three interacting QDs coupled to the reservoir [36–38]. For simplicity, on-site Coulomb repulsion was considered only in a single QD. Such a model is suitable in the case where one of the dots is narrow and the second is rather wide. In [39, 40], the authors derived rate equations to analyze the case of resonant transport in QDs linked by ballistic channels with high density of states and revealed the role of interference effects.

In this paper, we consider charge relaxation in double QDs due to the coupling to the continuous spectrum states. Tunneling from the first QD to the continuum is possible only through the second dot. We obtain a closed system of equations for the time evolution of the localized-electron filling numbers that exactly takes all-order correlation functions for localized electrons into account. We decouple the higher-order correlation functions between conduction electrons in the reservoir (band electrons) and electrons localized in the QDs. In such an approximation, the electron distribution in the reservoir is not influenced by changing the electronic states in the coupled QDs. For QDs weakly coupled to the reservoir, the proposed decoupling scheme is a good approximation. We consider different initial charge configurations and take Coulomb correlations into account both within QDs and between electrons localized in different dots. We find some peculiarities in the dynamics of electron filling numbers arising due to the Coulomb correlation effects. We demonstrate that depending on the initial charge configurations, the effect of dynamical charge trapping can be observed in the proposed system.

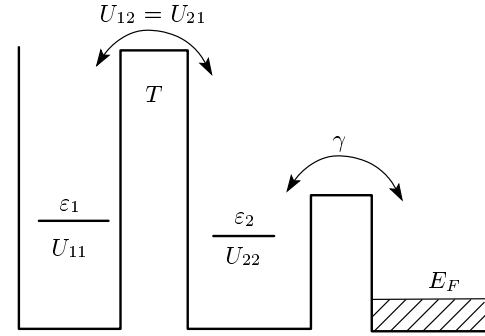


Fig. 1. Scheme of the proposed model. The system of interacting QDs is coupled to the continuous-spectrum states by the tunneling rate $\gamma = \pi\nu_0 t^2$

2. THE PROPOSED MODEL

We consider a system of coupled QDs with the single-particle levels ε_1 and ε_2 coupled to an electronic reservoir (Fig. 1). We discuss three different initial charge configurations that are possible in the proposed system. The first deals with the initial charge localized in the first QD on the energy level ε_1 ($n_{11\sigma}(0) = 1$). The second corresponds to the situation where localized charge is accumulated in the second QD on the energy level ε_2 ($n_{22\sigma}(0) = 1$). And the last possible initial charge configuration refers to the case where the initial charge is localized on both electron levels equally ($n_{11\sigma}(0) = n_{22\sigma}(0) = 1$). The second QD with the energy level ε_2 is connected with the continuous spectrum states (ε_p). Relaxation of the localized charge is governed by the Hamiltonian

$$\hat{H} = \hat{H}_D + \hat{H}_{tun} + \hat{H}_{res}. \quad (1)$$

The Hamiltonian \hat{H}_D of interacting QDs,

$$\begin{aligned} \hat{H}_D = & \\ = & \sum_{i=1,2\sigma} \varepsilon_i c_{i\sigma}^\dagger c_{i\sigma} + U_{11} n_{11\sigma} n_{11-\sigma} + U_{22} n_{22\sigma} n_{22-\sigma} + \\ & + U_{12} (n_{11\sigma} + n_{11-\sigma})(n_{22\sigma} + n_{22-\sigma}) + \\ & + \sum_{\sigma} T (c_{1\sigma}^\dagger c_{2\sigma} + c_{1\sigma} c_{2\sigma}^\dagger), \quad (2) \end{aligned}$$

contains the spin-degenerate levels ε_i (indices $i = 1$ and $i = 2$ correspond to the first and second QDs), the on-site Coulomb repulsion for the double occupation of the QDs, and Coulomb interaction between electrons in different dots. The creation/annihilation of an electron with spin $\sigma = \pm 1$ within a dot is denoted by $c_{i\sigma}^\dagger/c_{i\sigma}$ and n_σ is the corresponding filling number operator.

The coupling between the dots is described by the tunneling transfer amplitude T , which is assumed to be independent of momentum and spin.

The continuous-spectrum states are modeled by the Hamiltonian

$$\hat{H}_{res} = \sum_{p\sigma} \varepsilon_p c_{p\sigma}^\dagger c_{p\sigma}, \quad (3)$$

where $c_{p\sigma}^\dagger/c_{p\sigma}$ creates/annihilates an electron with spin σ and momentum p in the lead. The coupling between the second dot and the continuous-spectrum states is described by the Hamiltonian

$$\hat{H}_{tun} = \sum_{p\sigma} t(c_{p\sigma}^\dagger c_{2\sigma} + c_{p\sigma} c_{2\sigma}^\dagger), \quad (4)$$

where t is the tunneling amplitude, which we assume to be independent of momentum and spin. With a constant density of states, ν_0 assumed in the reservoir, the tunnel rate γ is defined as $\gamma = \pi\nu_0 t^2$.

Because we are interested in the specific features of the nonstationary time evolution of the initially localized charge in coupled QDs, we consider the situation where the condition $(\varepsilon_i - \varepsilon_F)/\gamma \gg 1$ is fulfilled. It means that the initial energy levels are situated well above the Fermi level and stationary occupation numbers in the second QD in the absence of coupling between the QDs is of the order of $\gamma/(\varepsilon_2 - \varepsilon_F) \ll 1$ and can be omitted. Consequently, the Kondo effect is also negligible in the proposed model.

Our investigation deals with the low-temperature regime where the Fermi level is well defined and the temperature is much lower than all typical relaxation rates in the system. Consequently, the distribution function of electrons in the leads (band electrons) is a Fermi step.

We set $\hbar = 1$, and therefore the kinetic equations for bilinear combinations of Heisenberg operators $c_{i\sigma}^\dagger/c_{i\sigma}$,

$$\begin{aligned} c_{1\sigma}^\dagger c_{1\sigma} &= \hat{n}_1^\sigma(t), & c_{2\sigma}^\dagger c_{2\sigma} &= \hat{n}_2^\sigma(t), \\ c_{1\sigma}^\dagger c_{2\sigma} &= \hat{n}_{12}^\sigma(t), & c_{2\sigma}^\dagger c_{1\sigma} &= \hat{n}_{21}^\sigma(t), \end{aligned} \quad (5)$$

which describe time evolution of the filling numbers for the electrons, can be written as

$$\begin{aligned} i \frac{\partial}{\partial t} \hat{n}_{11}^\sigma &= -T(\hat{n}_{21}^\sigma - \hat{n}_{12}^\sigma), \\ i \frac{\partial}{\partial t} \hat{n}_{22}^\sigma &= T(\hat{n}_{21}^\sigma - \hat{n}_{12}^\sigma) - 2i\gamma \hat{n}_{22}^\sigma, \\ i \frac{\partial}{\partial t} \hat{n}_{21}^\sigma &= T(\hat{n}_{22}^\sigma - \hat{n}_{11}^\sigma) + \\ &+ [\xi + (U_{11} - U_{21})\hat{n}_{11}^{-\sigma}] \hat{n}_{21}^\sigma - \\ &- (U_{22} - U_{12})\hat{n}_{21}^\sigma \hat{n}_{22}^{-\sigma} - i\gamma \hat{n}_{21}^\sigma, \\ i \frac{\partial}{\partial t} \hat{n}_{12}^\sigma &= -T(\hat{n}_{22}^\sigma - \hat{n}_{11}^\sigma) - \\ &- [\xi + (U_{11} - U_{21})\hat{n}_{11}^{-\sigma}] \hat{n}_{12}^\sigma + \\ &+ (U_{22} - U_{12})\hat{n}_{12}^\sigma \hat{n}_{22}^{-\sigma} - i\gamma \hat{n}_{12}^\sigma, \end{aligned} \quad (6)$$

where $\xi = \varepsilon_1 - \varepsilon_2$ is the detuning between the energy levels in the QDs. System of equations (6) contains expressions for the pair correlators $\hat{n}_1^{-\sigma} \hat{n}_{21}^\sigma$ and $\hat{n}_1^{-\sigma} \hat{n}_{12}^\sigma$, which also determine relaxation of the localized charge and consequently have to be evaluated. In this system, we neglect higher-order correlation functions between localized and continuous-spectrum (band) electrons and perform averaging over electron states in the reservoir.

We introduce the notation $K_{ijj'\sigma}^{\sigma\sigma'} = \langle c_{i\sigma}^\dagger c_{j\sigma} c_{j'\sigma'}^\dagger c_{i'\sigma'} \rangle$ for the pair correlators and consider only the paramagnetic case $\langle \hat{n}_i^\sigma \rangle = \langle \hat{n}_i^{-\sigma} \rangle$. Then the relations

$$\begin{aligned} K_{2111}^{\sigma-\sigma} &= \langle \hat{n}_{21}^\sigma \hat{n}_{11}^{-\sigma} \rangle = \langle \hat{n}_{21}^{-\sigma} \hat{n}_{11}^\sigma \rangle, \\ K_{1211}^{\sigma-\sigma} &= \langle \hat{n}_{12}^\sigma \hat{n}_{11}^{-\sigma} \rangle = \langle \hat{n}_{12}^{-\sigma} \hat{n}_{11}^\sigma \rangle, \\ K_{2122}^{\sigma-\sigma} &= \langle \hat{n}_{21}^\sigma \hat{n}_{22}^{-\sigma} \rangle = \langle \hat{n}_{21}^{-\sigma} \hat{n}_{22}^\sigma \rangle, \\ K_{1222}^{\sigma-\sigma} &= \langle \hat{n}_{12}^\sigma \hat{n}_{22}^{-\sigma} \rangle = \langle \hat{n}_{12}^{-\sigma} \hat{n}_{22}^\sigma \rangle \end{aligned} \quad (7)$$

hold. The system of equations for pair correlators can be written in the compact matrix form (symbol $[[$] means commutation and the symbol $\{ \}$ — anticommutation)

$$i \frac{\partial}{\partial t} \hat{K} = [\hat{K}, \hat{H}'] + \{ \hat{K}, \hat{\Gamma} \} + \hat{Y}, \quad (8)$$

where

$$\begin{aligned} \hat{K} &= \begin{pmatrix} K_{2211}^{\sigma-\sigma} & K_{1211}^{\sigma-\sigma} & K_{2221}^{\sigma-\sigma} & K_{1221}^{\sigma-\sigma} \\ K_{2111}^{\sigma-\sigma} & K_{1111}^{\sigma-\sigma} & K_{2121}^{\sigma-\sigma} & K_{1121}^{\sigma-\sigma} \\ K_{2212}^{\sigma-\sigma} & K_{1212}^{\sigma-\sigma} & K_{2222}^{\sigma-\sigma} & K_{1222}^{\sigma-\sigma} \\ K_{2112}^{\sigma-\sigma} & K_{1112}^{\sigma-\sigma} & K_{2122}^{\sigma-\sigma} & K_{1122}^{\sigma-\sigma} \end{pmatrix} = \\ &= ||K_{ij}|| \end{aligned} \quad (9)$$

is the pair correlators matrix,

$$\hat{H}' = \begin{pmatrix} 0 & T & T & 0 \\ T & \xi + U_{11} - U_{21} & 0 & T \\ T & 0 & -\xi + U_{22} - U_{12} & T \\ 0 & T & T & 0 \end{pmatrix}, \quad (10)$$

$$\hat{\Gamma} = \begin{pmatrix} -i\gamma & 0 & 0 & 0 \\ 0 & 0 & 0 & 0 \\ 0 & 0 & -2i\gamma & 0 \\ 0 & 0 & 0 & -i\gamma \end{pmatrix} \quad (11)$$

and

$$\hat{\Upsilon} = \begin{pmatrix} 0 & U_2 K_{121122}^{\sigma-\sigma-\sigma} & U_1 K_{211122}^{\sigma-\sigma-\sigma} & 0 \\ -U_2 K_{211122}^{\sigma-\sigma-\sigma} & 0 & 0 & -U_2 K_{211122}^{\sigma-\sigma-\sigma} \\ -U_1 K_{121122}^{\sigma-\sigma-\sigma} & 0 & 0 & -U_1 K_{121122}^{\sigma-\sigma-\sigma} \\ 0 & U_2 K_{121122}^{\sigma-\sigma-\sigma} & U_1 K_{211122}^{\sigma-\sigma-\sigma} & 0 \end{pmatrix}, \quad (12)$$

where $U_1 = U_{11} - U_{21}$ and $U_2 = U_{22} - U_{12}$.

When evolution starts from the state with the charge in the first QD and with the second QD empty, system of equations (8) for pair correlators satisfies the initial conditions $K_{1111}^{\sigma-\sigma}(0) = 1$, $K_{2222}^{\sigma-\sigma}(0) = 0$, and $K_{ij'j'}^{\sigma-\sigma}(0) = 0$ for the other combinations of indices i, j . If we are interested in the case where all the initial charge in the system is localized in the second QD, system of equations (8) for pair correlators satisfies the initial conditions $K_{2222}^{\sigma-\sigma}(0) = 1$, $K_{1111}^{\sigma-\sigma}(0) = 0$, and $K_{ij'j'}^{\sigma-\sigma}(0) = 0$ for the other combinations of indices i, j . In the case where the initial charge is equally distributed between the dots, system of equations (8) for pair correlators satisfies the initial conditions

$$K_{1111}^{\sigma-\sigma}(0) = K_{2222}^{\sigma-\sigma}(0) = K_{1122}^{\sigma-\sigma}(0) = 1, \quad K_{ij'j'}^{\sigma-\sigma}(0) = 0$$

for the other combinations of indices i, j .

The higher-order correlators $K_{121122}^{\sigma-\sigma-\sigma}$ and $K_{211122}^{\sigma-\sigma-\sigma}$ are exactly equal to zero because they are the solution of a linear homogeneous system of equations with zero initial conditions. Consequently, system of equations (6), (8), which determines the localized charge evolution in coupled QDs connected with the reservoir, can be solved numerically. The obtained results for all the initial conditions are discussed in Sec. 3.

2.1. Analytic solution for time-dependent filling numbers

We now focus on the specific configuration of the proposed system, which allows obtaining an analytic

are the tunneling coupling matrices.

We can easily see that Eqs. (8) contain expressions for the higher-order correlators $K_{121122}^{\sigma-\sigma-\sigma}$ and $K_{211122}^{\sigma-\sigma-\sigma}$. Their contribution can be easily written in the matrix form

solution. In this section, we discuss only the situation where at the initial time two electrons with opposite spins are localized only in the first QD on the energy level ε_1 ($n_{1\sigma}(0) = n_0 = 1$). Moreover, we consider the Coulomb interaction only in the first QD for simplicity. Such a model is suitable in the case where the first QD is narrow and the second is rather wide [37, 41]. Besides, if electrons are initially located in the first QD and the second dot is empty, then filling numbers for the electrons in the second QD remain rather small during the time evolution of the charge and Coulomb effects in the second QD are not so important as in the first one. Moreover, Coulomb interaction in the second QD does not lead to an essentially new physics. It can be treated by a rather simple renormalization of detuning: ξ has to be substituted by $\tilde{\xi} = \xi - U_{22} + U_{12}$ and the Coulomb coupling in the first QD, U_{11} , has to be substituted by $\tilde{U}_{11} = U_{11} + U_{22} - 2U_{12}$.

The formal solution of the system for pair correlators (see Eq. (8)) can be written using the evolution operator. Time evolution of the matrix elements K_{ij} (see Eq. (9)) is given by the expression

$$K_{ij}(t) = \sum_{mn} (e^{-i\hat{H}t})_{im} K_{mn}(0) (e^{i\hat{H}t})_{nj}, \quad (13)$$

where $\hat{H} = \hat{H}' + \hat{\Gamma}$.

We introduce the evolution operator

$$\Phi_{ij}(t) = (e^{-i\hat{H}t})_{ij}. \quad (14)$$

The time evolution of the pair correlators can then be found from the expressions

$$\begin{aligned}
 K_{2111}^{\sigma-\sigma} &= (e^{-i\hat{H}t})_{12}K(0)_{22}(e^{i\hat{H}^\dagger t})_{22} = \\
 &= \Phi_{12}(t)\tilde{\Phi}_{22}(t), \\
 K_{1211}^{\sigma-\sigma} &= (e^{-i\hat{H}t})_{22}K(0)_{22}(e^{i\hat{H}^\dagger t})_{21} = \\
 &= \Phi_{22}(t)\tilde{\Phi}_{21}(t),
 \end{aligned} \tag{15}$$

since $K(0)_{22}$ in the matrix (see Eq. (9)) is equal to $K_{1111}^{\sigma-\sigma}(0) = 1$. The evolution operator $\tilde{\Phi}_{22}(t)$ can be obtained from the operator $\Phi_{22}(t)$ by the substitutions $t \rightarrow -t$ and $\gamma \rightarrow -\gamma$. The pair correlator $K_{1211}^{\sigma-\sigma}$ is a complex conjugate of $K_{2111}^{\sigma-\sigma}$.

Finally, the evolution operators $\Phi_{ij}(t)$ are determined by the equations

$$\begin{pmatrix} i\frac{\partial}{\partial t}\Phi_{12}(t) \\ i\frac{\partial}{\partial t}\Phi_{22}(t) \\ i\frac{\partial}{\partial t}\Phi_{32}(t) \\ i\frac{\partial}{\partial t}\Phi_{42}(t) \end{pmatrix} = \hat{H} \begin{pmatrix} \Phi_{12}(t) \\ \Phi_{22}(t) \\ \Phi_{32}(t) \\ \Phi_{42}(t) \end{pmatrix}, \tag{16}$$

with the initial conditions

$$\Phi_{ij}(0) = \delta_{ij}. \tag{17}$$

The characteristic equation for the eigenvalues λ_i of the evolution operator $\Phi_{ij}(t)$ has the form

$$\begin{aligned}
 (H_{11} - \lambda)(H_{22} - \lambda)(H_{33} - \lambda)(H_{44} - \lambda) - \\
 - T^2[(H_{11} - \lambda)(H_{22} - \lambda) + (H_{11} - \lambda)(H_{33} - \lambda) + \\
 + (H_{33} - \lambda)(H_{44} - \lambda) + (H_{22} - \lambda)(H_{44} - \lambda)] = 0,
 \end{aligned} \tag{18}$$

where

$$\begin{aligned}
 H_{11} &= H_{44} = -i\gamma, \\
 H_{22} &= \xi + U_{11}, \\
 H_{33} &= -\xi - 2i\gamma.
 \end{aligned} \tag{19}$$

Each eigenvalue λ_i determines the corresponding eigenvector

$$\psi_i = \begin{pmatrix} \alpha_i \\ \beta_i \\ \gamma_i \\ \delta_i \end{pmatrix}. \tag{20}$$

We have to obtain expressions for the evolution operators $\Phi_{12}(t)$ and $\Phi_{22}(t)$ with the initial conditions $\Phi_{22}(0) = 1$ and $\Phi_{ij}(0) = 0$.

The solution of the system of equations for $\Phi_{12}(t)$ and $\Phi_{22}(t)$ can be written as

$$\begin{aligned}
 \Phi_{12}(t) &= \sum_{i=1}^4 C_i \alpha_i \exp(-i\lambda_i t), \\
 \Phi_{22}(t) &= \sum_{i=1}^4 C_i \beta_i \exp(-i\lambda_i t),
 \end{aligned} \tag{21}$$

where the constants C_i can be obtained from the initial conditions for the system of equations:

$$\begin{aligned}
 \sum_i C_i \alpha_i &= 0, \\
 \sum_i C_i \beta_i &= 1, \\
 \sum_i C_i \gamma_i &= 0, \\
 \sum_i C_i \delta_i &= 0.
 \end{aligned} \tag{22}$$

2.2. Equations for time-dependent filling numbers

The time-dependent filling numbers $n_1(t)$ can be found from the inhomogeneous part of Eqs. (6), which gives

$$\begin{aligned}
 \left\{ \left[\left(i\frac{\partial}{\partial t} + i\gamma \right)^2 + \gamma^2 \right] \left[\left(i\frac{\partial}{\partial t} + i\gamma \right)^2 - \xi^2 \right] - \right. \\
 \left. - 4T^2 \left(i\frac{\partial}{\partial t} + i\gamma \right)^2 \right\} n_1(t) = \left(i\frac{\partial}{\partial t} + 2i\gamma \right) \times \\
 \times T [U_1(G_2^{-1}K_{1211}^{\sigma-\sigma} + G_1^{-1}K_{2111}^{\sigma-\sigma}) - \\
 - U_2(G_2^{-1}K_{2111}^{\sigma-\sigma} + G_1^{-1}K_{2122}^{\sigma-\sigma})],
 \end{aligned} \tag{23}$$

where

$$\begin{aligned}
 G_2^{-1} &= i\frac{\partial}{\partial t} + \xi + i\gamma, \\
 G_1^{-1} &= i\frac{\partial}{\partial t} - \xi + i\gamma.
 \end{aligned} \tag{24}$$

The solution of the Eq. (23) describes localized charge relaxation and consists of the two parts: the first is the general solution of the homogeneous equation $n_1^h(t)$ (the right-hand side is equal to zero) and the second is a particular solution, $\tilde{n}_1(t)$, of the inhomogeneous equation:

$$\begin{aligned}
 n_1(t) &= n_1^h(t) + \tilde{n}_1(t) = \\
 &= n_1^h(t) + \int_0^t G(t-t')P(t') dt',
 \end{aligned} \tag{25}$$

where $G(t - t')$ is the Green's function of Eq. (23) with $\delta(t - t')$ in the right-hand side and $P(t')$ is the right-hand side of Eq. (23), which appears due to the Coulomb correlations.

The general solution of the homogeneous equation has the form [36]

$$n_1^h(t) = n_1^0[A' \exp(-i(E_1 - E_1^*)t) + 2 \operatorname{Re}(B' \exp(-i(E_1 - E_2^*)t)) + C' \exp(-i(E_2 - E_2^*)t)], \quad (26)$$

where

$$A' = \frac{|E_2 - \varepsilon_1|^2}{|E_2 - E_1|^2}, \quad C' = \frac{|E_1 - \varepsilon_1|^2}{|E_2 - E_1|^2}, \quad (27)$$

$$B' = -\frac{(E_2 - \varepsilon_1)(E_1^* - \varepsilon_1)}{|E_2 - E_1|^2}.$$

The eigenfrequencies E_i can be found from the equation

$$(E - \varepsilon_1)(E - \varepsilon_2 + i\gamma) - T^2 = 0, \quad (28)$$

and are given by

$$E_{1,2} = \frac{1}{2}(\varepsilon_1 + \varepsilon_2 - i\gamma) \pm \frac{1}{2}\sqrt{(\varepsilon_1 - \varepsilon_2 + i\gamma)^2 + 4T^2}. \quad (29)$$

The Green's function $G(t - t')$ of Eq. (23) can be written as

$$G(t - t') = \sum_{i=1}^4 a_i \exp(-i\lambda_i(t - t')) \Theta(t - t'), \quad (30)$$

and consequently, the particular solution of the inhomogeneous equation has the form

$$\tilde{n}_1(t) = \sum_{ijk} a_i C_j \exp(-\lambda_i t) \frac{1}{-i(\lambda_j - \lambda_k^* - \lambda_i)} \times [\exp(-i(\lambda_j - \lambda_k^* - \lambda_i)t) - 1], \quad (31)$$

where $\lambda_{j(k)}$ can be found from Eq. (18) and λ_i are the roots of the characteristic equation arising from Eq. (23):

$$\lambda_{1,2} = -i\gamma \pm \left[\frac{4T^2 + \xi^2 - \gamma^2}{2} + \frac{1}{2}\sqrt{(4T^2 + \xi^2 - \gamma^2)^2 + 4\xi^2\gamma^2} \right]^{1/2}, \quad (32)$$

$$\lambda_{3,4} = -i\gamma \pm \left[\frac{4T^2 + \xi^2 - \gamma^2}{2} - \frac{1}{2}\sqrt{(4T^2 + \xi^2 - \gamma^2)^2 + 4\xi^2\gamma^2} \right]^{1/2}.$$

These roots are related to the eigenfrequencies E_i as

$$\begin{aligned} \lambda_{1,2} &= E_{1,2} - E_{1,2}^*, \\ \lambda_3 &= E_1 - E_2^*, \\ \lambda_4 &= E_2 - E_1^*. \end{aligned} \quad (33)$$

The coefficients a_i are

$$\begin{aligned} a_1 &= \frac{1}{(\lambda_2 - \lambda_1)(\lambda_3 - \lambda_1)(\lambda_4 - \lambda_1)}, \\ a_2 &= \frac{1}{(\lambda_1 - \lambda_2)(\lambda_3 - \lambda_2)(\lambda_4 - \lambda_2)}, \\ a_3 &= \frac{1}{(\lambda_1 - \lambda_3)(\lambda_2 - \lambda_3)(\lambda_4 - \lambda_3)}, \\ a_4 &= \frac{1}{(\lambda_1 - \lambda_4)(\lambda_2 - \lambda_4)(\lambda_3 - \lambda_4)}. \end{aligned} \quad (34)$$

We now focus on the two limit cases where the expressions that determine the dynamics of the filling numbers have a rather compact form. The first case is where the detuning between the empty energy levels in the QDs is equal to zero: $\xi/\gamma \ll 1$. The second case deals with the situation where the sum of the detuning and half the Coulomb coupling value is equal to zero. This means that the resonance between the half-occupied energy level in the first QD and the empty level in the second QD occurs:

$$\frac{\xi + U_{11}/2}{\gamma} \ll 1.$$

We also assume that the condition $T \ll \gamma \ll U_{11}$ is fulfilled in both cases.

2.3. $\xi/\gamma \ll 1$

The eigenvalues of the characteristic equation in the first case ($\xi/\gamma \ll 1$), to within T^2/U_{11}^2 have the form

$$\begin{aligned} \lambda_1 &= U_{11} - i\frac{2T^2\gamma}{U^2}, \\ \lambda_2 &= -i\gamma - i\frac{2T^2}{\gamma}, \\ \lambda_3 &= -2i\gamma - i\frac{2T^2}{\gamma}, \\ \lambda_4 &= -i\gamma. \end{aligned} \quad (35)$$

Hence, the evolution operators can be written as

$$\begin{aligned} \Phi_{12}(t) &= \frac{T}{U_{11}} \left[\exp \left(-iU_{11}t - \frac{2T^2\gamma}{U_{11}^2}t \right) - \right. \\ &\quad \left. - \exp \left(-\gamma t - \frac{2T^2}{\gamma}t \right) \right], \\ \Phi_{22}(t) &= \left(1 - \frac{2T^2}{U^2} \right) \exp \left(-iU_{11}t - \frac{2T^2\gamma}{U_{11}^2}t \right) + \\ &\quad + \frac{2T^2}{U_{11}^2} \exp \left(-\gamma t - \frac{2T^2}{\gamma}t \right), \end{aligned} \quad (36)$$

and time dependence of the pair correlators $K_{2111}^{\sigma-\sigma}$ and $K_{1211}^{\sigma-\sigma}$ is determined by the product

$$\begin{aligned} K_{2111}^{\sigma-\sigma}(t) &= \Phi_{12}(t)\Phi_{22}^*(t), \\ K_{1211}^{\sigma-\sigma}(t) &= (K_{2111}^{\sigma-\sigma})^*. \end{aligned} \quad (37)$$

The expression for $P(t)$ (see Eq. (25)) in the case of the resonance between empty levels, $\xi/\gamma = 0$, has the form

$$\begin{aligned} P(t) &= 4T^2\gamma \exp \left(-\frac{4T^2\eta}{\gamma}t \right) + \\ &\quad + 2T^2U_{11} \exp(-\gamma t) \cos(U_{11}t), \end{aligned} \quad (38)$$

where $\eta = \gamma^2/(U_{11}^2 + \gamma^2)$. For $\eta = 1/2$, the inhomogeneous part of the time evolution of the filling numbers $\tilde{n}_1(t)$ can be written as

$$\begin{aligned} \tilde{n}_1(t) &= \frac{T^2}{\gamma^2} \left[\left(-2\gamma t - \exp \left(-\frac{2T^2}{\gamma}t \right) \right) \times \right. \\ &\quad \times \exp \left(-\frac{2T^2}{\gamma}t \right) + \exp(-2\gamma t) + \\ &\quad \left. + 4 \exp \left(-\frac{2T^2}{\gamma}t \right) - 4 \exp(-\gamma t) \right] + \\ &\quad + \frac{2T^2U_{11} \exp(-\gamma t)}{\gamma^3} [\cos(U_{11}t) - 1] + \\ &\quad + O \left(\frac{T^2}{U_{11}^2} \frac{\gamma}{U_{11}} \right). \end{aligned} \quad (39)$$

For $\eta \ll 1$, the time evolution of the filling numbers $\tilde{n}_1(t)$ is given by

$$\begin{aligned} \tilde{n}_1(t) &= \frac{1}{1-2\eta} \left[\exp \left(-4\frac{T^2\eta}{\gamma}t \right) - \exp \left(-\frac{2T^2}{\gamma}t \right) \right] + \\ &\quad + O \left(\frac{T^2}{\gamma^2} \right). \end{aligned} \quad (40)$$

2.4. $(\xi + U_{11}/2)/\gamma \ll 1$

In the second case of interest ($(\xi + U_{11}/2)/\gamma \ll 1$ but $U_{11}/\gamma \gg 1$), the eigenvalues are

$$\begin{aligned} \lambda_1 &= \frac{U_{11}}{2} - i\frac{8T^2\gamma}{U_{11}^2}, \\ \lambda_2 &= -i\gamma + \frac{8T^2}{U_{11}}, \\ \lambda_3 &= -2i\gamma + \frac{U_{11}}{2} - \frac{i8T^2\gamma}{U_{11}^2} + \frac{4T^2}{U_{11}}, \\ \lambda_4 &= -i\gamma. \end{aligned} \quad (41)$$

The evolution operators take the form

$$\begin{aligned} \Phi_{12}(t) &= \frac{2T}{U_{11}} \times \\ &\quad \times \left[\exp \left(-i\frac{U_{11}}{2}t - \frac{8T^2\gamma}{U_{11}^2}t \right) - \exp(-\gamma t) \right], \\ \Phi_{22}(t) &= \left(1 - \frac{8T^2}{U_{11}^2} \right) \exp \left(-i\frac{U_{11}}{2}t - \frac{8T^2\gamma}{U_{11}^2}t \right) + \\ &\quad + \frac{8T^2}{U_{11}^2} \exp(-\gamma t). \end{aligned} \quad (42)$$

When the condition $(\xi + U_{11}/2)/\gamma = 0$ is fulfilled, $P(t)$ is determined by the expression

$$\begin{aligned} P(t) &= -T^2U_{11}^2 \left(\exp \left(i\frac{U_{11}}{2}t - \gamma t \right) + \text{h.c.} \right) - \\ &\quad - 4T^2\gamma^2 \exp \left(-\frac{16T^2\gamma}{U_{11}^2}t \right) \end{aligned} \quad (43)$$

to within T^3/U_{11}^3 and γ^2/U_{11}^2 .

The inhomogeneous part of the time evolution of the filling numbers $\tilde{n}_1(t)$, to within T^2/U_{11}^2 , has the form

$$\begin{aligned} \tilde{n}_1(t) &= -\frac{4}{7} \left[1 - \exp \left(-14\frac{T^2\gamma}{U_{11}^2}t \right) \right] \exp \left(-\frac{2T^2\gamma}{U_{11}^2}t \right) - \\ &\quad - 2\frac{T^2}{\gamma U_{11}} \exp(-\gamma t) \sin \left(\frac{U_{11}}{2}t \right) + O \left(\frac{T^2}{U_{11}^2} \right). \end{aligned} \quad (44)$$

We note that relaxation of the filling numbers in the proposed model can be analyzed by means of a simpler method, the self-consistent mean-field approximation [37, 42, 43]. In this approximation, the correlation functions $U_{11}\langle \hat{n}_i^{-\sigma} \hat{n}_{ij}^{\sigma} \rangle$ in Eqs. (6) are substituted by the expressions $U_{11}\langle \hat{n}_i^{-\sigma} \rangle \langle \hat{n}_{ij}^{\sigma} \rangle$. This substitution is valid in the case where filling numbers for the localized electrons $n_i^{-\sigma}$ change their values rather slowly. The calculation scheme consists of two steps. In the first step, the initial energy level position ε_i is replaced by the expression

$$\tilde{\varepsilon}_i = \varepsilon_i + U_{11}\langle \hat{n}_i^{-\sigma} \rangle$$

and the time-dependent filling numbers are evaluated. The second step deals with the self-consistent calculation of the time-dependent filling numbers for the electrons. For some ranges of the system parameters, the mean-field approximation reveals qualitatively good results [37]. But in general case, the mean-field approximation is insufficient to describe relaxation processes in systems with correlations.

3. MAIN RESULTS AND DISCUSSION

Time evolution of the electron filling numbers strongly depends on the initial charge configuration of the system and on the relations between the system parameters (energy levels positions, the difference of Coulomb interaction between various localized states, and the relations between tunneling rates). We consider the situation where $T < \gamma < U_{ij}$.

We first analyze the situation where all the charge in the system is localized in the first QD at the initial time instant and the second QD is empty (see Fig. 2 and Fig. 3*a,d*). In what follows, we discuss the case of both positive (see Fig. 2) and negative (see Fig. 3*a,d*) initial detunings ξ . We start from the energy level configuration with positive detuning. Figure 2*a* demonstrates the decrease in the localized charge relaxation rate in the first QD with the increase in the Coulomb coupling values (the grey line and the black dashed line) in comparison with the case where Coulomb interaction is absent (black line). This effect occurs because the presence of strong Coulomb repulsion results in an increase in the initial detuning value. Simultaneously, the increase in Coulomb coupling values leads to a decrease in the filling number amplitudes in the second QD (see Fig. 2*b*). Time evolution of the filling numbers demonstrates several typical time intervals with extremely different values of relaxation rates if $\xi/\gamma < 1$. At the first stage, relaxation occurs with the rate very close to $\gamma_{res} = 2T^2/\gamma$. This stage also demonstrates the increase in the filling number amplitudes in the second dot (see Fig. 2*b*). Further time evolution in both dots reveals a decrease in the charge amplitude, which occurs with the typical relaxation rate very close to

$$\gamma_{nonres} = \gamma_{res} \frac{\gamma^2}{\gamma^2 + \xi^2}.$$

The energy-level configuration that corresponds to the negative initial detuning reveals much more interesting results (see Fig. 3*a,d*). It can be found that critical Coulomb coupling values exist in the system for a given set of parameters that corresponds to the relaxation regime changing. For the values smaller than the

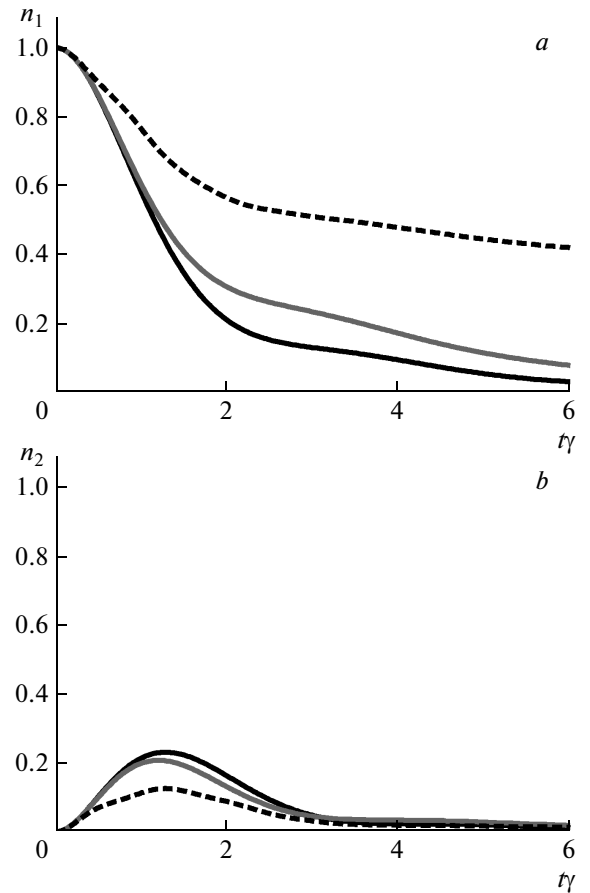


Fig. 2. Time evolution of filling numbers in the presence of Coulomb interaction in the case of a positive initial detuning ξ/γ in the first (a) and the second (b) QD. The initial charge is localized in the first QD ($n_1(0) = 1$, $n_2(0) = 0$). The black line corresponds to the case where $U_{11}/\gamma = 0$, $U_{12}/\gamma = U_{21}/\gamma = 0$, and $U_{22}/\gamma = 0$; the grey line describes the situation where $U_{11}/\gamma = 2.0$, $U_{12}/\gamma = U_{21}/\gamma = 1.2$; and $U_{22}/\gamma = 1.5$; and the black dashed line, the case where $U_{11}/\gamma = 10.0$, $U_{12}/\gamma = U_{21}/\gamma = 4.0$, and $U_{22}/\gamma = 8.0$. For all figures the parameter values $T/\gamma = 0.6$, $\gamma = 1.0$, and $\xi/\gamma = 0.8$ are the same

critical one, Coulomb interaction results in an increase in the localized charge relaxation rate in the first QD and leads to an increasing in filling number amplitudes in the second dot in comparison with the case where Coulomb interaction is absent (see Fig. 3*a,d* black and grey lines).

For the on-site Coulomb repulsion values larger than the critical one, the localized charge time evolution reveals a decrease in both the localized charge relaxation rate in the first QD and the filling-number

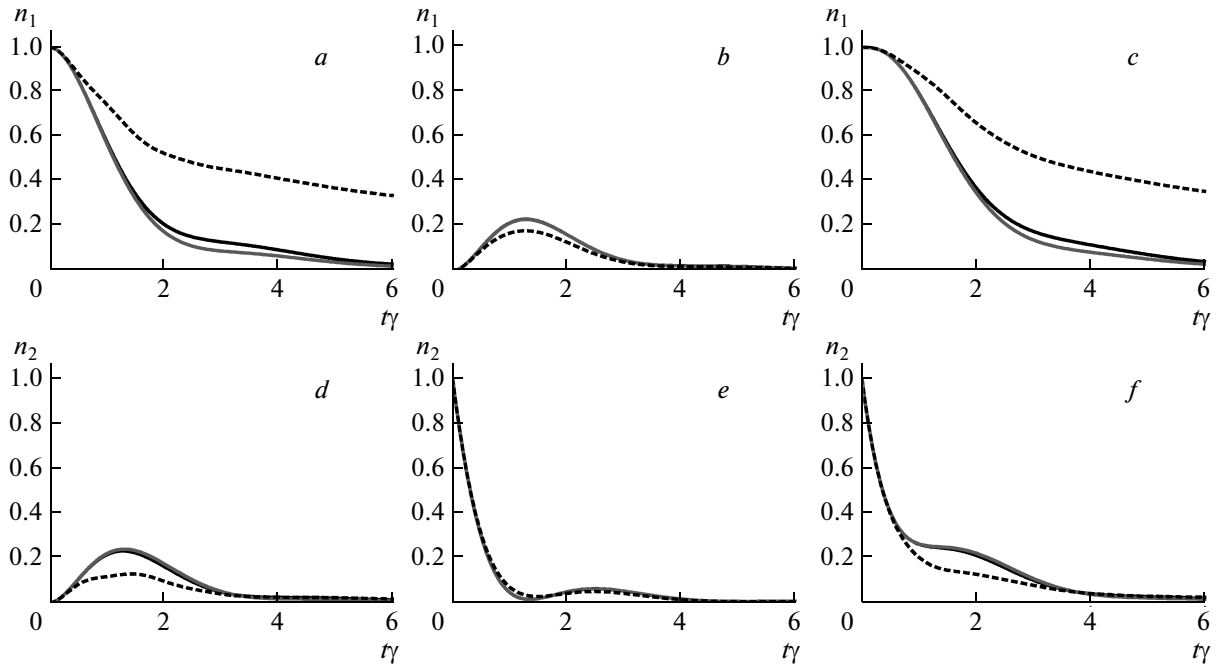


Fig. 3. Time evolution of filling numbers in the presence of Coulomb interaction in the case of a negative initial detuning ξ/γ : in the first (*a-c*) and in the second QD (*d-f*). The black line corresponds to the case where $U_{11}/\gamma = 0$, $U_{12}/\gamma = U_{21}/\gamma = 0$, and $U_{22}/\gamma = 0$; the grey line describes the situation where $U_{11}/\gamma = 1.8$, $U_{12}/\gamma = U_{21}/\gamma = 1.3$, and $U_{22}/\gamma = 1.5$, and the black dashed line, the case where $U_{11}/\gamma = 10.0$, $U_{12}/\gamma = U_{21}/\gamma = 4.0$, and $U_{22}/\gamma = 8.0$. *a* and *d*: the initial charge is localized in the first QD ($n_1(0) = 1$, $n_2(0) = 0$); *b* and *e*: the initial charge is localized in the second QD ($n_1(0) = 0$, $n_2(0) = 1$); *c* and *f*: the initial charge is localized in the both QDs ($n_1(0) = 1$, $n_2(0) = 1$). For all figures, the parameter values $T/\gamma = 0.6$, $\gamma = 1.0$, and $\xi/\gamma = -0.8$ are the same

amplitudes in the second one in comparison with the case where Coulomb repulsion is absent (see Fig. 3*a,d* black and black dashed lines). This is the result of the positive effective detuning formation; consequently, for large values of Coulomb interaction, relaxation reveals a behavior very similar to the case with a positive initial detuning (Fig. 2). Moreover, the typical relaxation rates are very close to the rate obtained for the energy-level configuration with positive detuning.

We now focus on the situation where all the initial charge in the system is localized in the second QD at the initial time instant and the first dot is empty (see Fig. 3*b,e*). The system behavior is then very similar for positive and negative detunings, and we therefore focus only on the case of negative initial detuning. The influence of Coulomb interaction on the localized charge relaxation in the case of both positive and negative initial detunings is negligible in comparison with the case where Coulomb repulsion is absent. Coulomb correlations modify the filling number time evolution only slightly, and relaxation occurs with the typical rate value close to γ . Due to the possibility of direct tun-

neling from the second QD to the continuous-spectrum states, the localized charge amplitude decreases faster than in the case where all the charge is localized in the first dot (see Fig. 3*a,e*).

The most interesting situation is shown in Fig. 3*c,f*. Calculation results correspond to the case where the localized charge is equally distributed between the dots at the initial time instant. We first describe the most interesting features of relaxation process that are valid both in the presence and in the absence of on-site Coulomb repulsion and occur for both values of the initial detuning.

Time evolution of the localized charge in both QDs reveals three typical time intervals with different values of the relaxation rate. The first time interval in the first QD demonstrates a plateau on the time interval of the order of γ . This interval demonstrates that the charge is still entirely localized in the first QD, because the second dot is occupied. The charge starts to flow from the first dot to the second one only when the second-dot energy level becomes nearly half empty due to the direct tunneling from the second dot to the continuous-

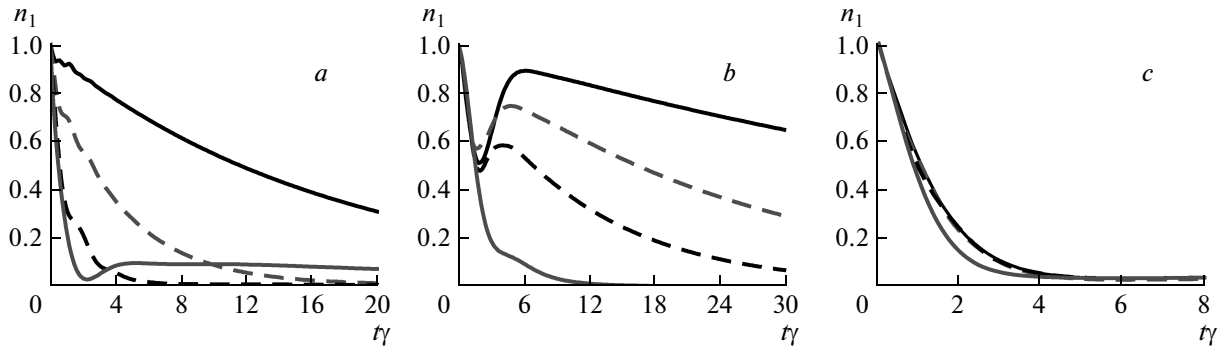


Fig. 4. Different time evolution regimes of the filling numbers $n_1(t)$ in the first QD in the presence of Coulomb interaction. *a)* $(\xi + U_1 - U_2)/\gamma = 0$ ($(U_1 - U_2)/\gamma = 10$ and $\xi/\gamma = -10$, black line; $(U_1 - U_2)/\gamma = 5$ and $\xi/\gamma = -5$, grey dashed line; $(U_1 - U_2)/\gamma = 3$ and $\xi/\gamma = -3$, black dashed line; $(U_1 - U_2)/\gamma = 1$ and $\xi/\gamma = -1$, grey line); *b)* $(\xi + U_1 - U_2)/\gamma \sim 1$ ($(U_1 - U_2)/\gamma = 10$ and $\xi/\gamma = -7$, black line; $(U_1 - U_2)/\gamma = 5$ and $\xi/\gamma = -4$, grey dashed line; $(U_1 - U_2)/\gamma = 3$ and $\xi/\gamma = -2.5$, black dashed line; $(U_1 - U_2)/\gamma = 1$ and $\xi/\gamma = -0.75$, grey line); *c)* $\xi/\gamma = 0$ ($U/\gamma = 10$, black line; $(U_1 - U_2)/\gamma = 5$, grey dashed line; $(U_1 - U_2)/\gamma = 3$, black dashed line; $(U_1 - U_2)/\gamma = 1$, grey line). The parameters $T/\gamma = 0.6$ and $\gamma = 1$ are the same for all figures

spectrum states. When both QDs are occupied by two electrons with opposite spins, charge transfer between the dots is forbidden due to the Pauli principle. Hence, at the first stage of relaxation, the charge in the first QD is trapped even in the absence of Coulomb correlations. On-site Coulomb repulsion results in a more dramatic charge redistribution between the QDs, which can be seen in Fig. 3*c,f*. The charge time evolution in the second QD occurs with the typical relaxation rate very close to γ .

The second time interval is connected with the formation of a plateau in the filling-number time evolution in the second QD. The time interval that determines the plateau is of the order of γ . This interval corresponds to the process of relaxation, and the rates consequently change in both dots. The next time interval demonstrates localized charge relaxation in both QDs with the typical relaxation rate very close to

$$\gamma_{nonres} = \gamma_{res} \frac{\gamma^2}{\gamma^2 + \xi^2}.$$

This time interval corresponds to the situation where both dots are nearly empty. Consequently, filling number relaxation in both QDs occurs with strongly different relaxation rates when the charge is mostly confined in the dots.

We next discuss the localized charge time evolution in the regime where the condition $(\xi + U_1 - U_2)/\gamma \ll 1$ is fulfilled. In this case, the increasing in the Coulomb coupling value leads to a decrease in the filling-number relaxation rate (see Fig. 4*a*). For large $U_1 - U_2$, the relaxation rate is rather low and is of the order of

$$\gamma_{nonres} = 2 \frac{T^2 \gamma}{(U_1 - U_2)^2},$$

which is typical for the system of two coupled QDs without Coulomb interaction and with $|\xi| \approx U_1 - U_2$. By the decreasing the Coulomb coupling value $U_1 - U_2$, we achieve the situation of resonant tunneling between the localized states, and consequently the relaxation rate increases. In Fig. 4*c*, the situation of resonant tunneling between empty energy levels $\xi/\gamma = 0$ is demonstrated. In this case, the relaxation of the localized charge occurs with the typical rate very close to the value $\gamma_{res} = 2T^2/\gamma$ and is almost independent of the Coulomb interaction value. We note that relaxation processes are governed not only by the typical exponentials $\exp(-\gamma t)$ and $\exp(-2T^2 t/\gamma)$ but also by the preexponential factor, which linearly increases in time in the resonant case (see Eq. (39)).

A very special relaxation regime exists in the system if the condition

$$\frac{\xi + U_1 - U_2}{\gamma} \sim 1$$

holds (see Fig. 4*b*). In this regime, Coulomb correlations result in formation of a dip in the time evolution of the localized charge. At the initial relaxation stage, the charge in the first QD rapidly decreases due to the almost resonant relation between the level in the second QD and the effective single-electron energy in the first dot. It follows from the third and the fourth equations in (6) that changing of the effective energy level detuning is determined by

$$(U_1 - U_2) \operatorname{Re} \left[\frac{\langle \hat{n}_1^{-\sigma}(t) \hat{n}_{12}^{\sigma}(t) \rangle}{\langle \hat{n}_{12}^{\sigma}(t) \rangle} \right],$$

which differs from the typical mean-field expression $(U_1 - U_2) \langle \hat{n}_i^{-\sigma}(t) \rangle$ [42].

At a certain instant of time the effective single-electron level falls down below the level in the second QD. At this instant, the inverse charge begins to flow from the second QD to the first one. The occupation in the first QD demonstrates a significant increase after reaching the minimum value (the dip formation). Filling numbers almost reach the initial value for large values of Coulomb interaction. After the dip formation, the typical time scale that determines relaxation of the filling numbers is sufficiently close to the value

$$\gamma_{nonres} = 2 \frac{T^2 \gamma}{\xi^2}.$$

This explanation gives a qualitative picture of the dip formation. The exact solution shows that Coulomb correlations are responsible for such nonmonotonic behavior. This effect is determined by the inhomogeneous part of the exact solution for time evolution of the filling numbers in the first QD (see the first term in Eq. (44)). And this inhomogeneous part appears because time dependence of the higher-order correlators ($P(t)$ in Eq. (23) and Eq. (25)) is completely taken into account. That is why time evolution of the filling numbers for the electrons differs considerably from that in the mean-field approximation. The width of the dip can be roughly estimated as $(1/8)\gamma_{nonres}^{-1}$.

Comparison between the exact solution and the mean-field approximation is demonstrated in Figs. 5, 6. It is clear that both methods reveal similar peculiarities of the system behavior such as several time ranges with considerably different relaxation rates. For some ranges of the system parameters, formation of the dip can also be reproduced in the mean-field approximation (see Fig. 5). Figure 5 also demonstrates similar behavior of the exact and mean-field solutions at the initial stage of relaxation. But the dip is reproduced incorrectly in the mean-field approximation.

In the case of resonant tunneling between the energy levels in the QDs ($\xi/\gamma = 0$), the exact solution and the mean-field approximation reveal a strong mismatch (see Fig. 6a). The exact solution demonstrates rather smooth time evolution of the localized charge, while the solution obtained by means of the mean-field approximation reveals abrupt changes in the localized charge amplitude. As the Coulomb repulsion decreases, the correspondence between the exact and the mean-field solutions improves (see Fig. 6b).

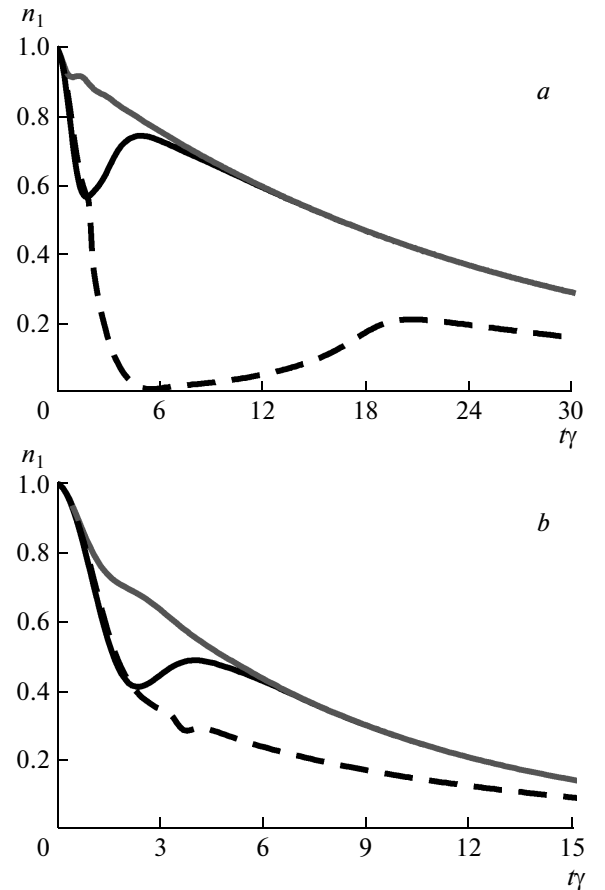


Fig. 5. Time dependence of the filling numbers for the electrons $n_1(t)$ in the presence of Coulomb interaction: comparison of the exact solution and the mean-field approximation. The black lines correspond to the exact solution, the black dashed lines correspond to the mean-field approximation. The grey lines demonstrate relaxation of the localized charge in the absence of Coulomb interaction. *a)* $(U_1 - U_2)/\gamma = 5$ and $\xi/\gamma = -3$; *b)* $(U_1 - U_2)/\gamma = 3$ and $\xi/\gamma = -2$. The parameters $T/\gamma = 0.6$ and $\gamma = 1$ are the same for all figures

4. CONCLUSION

We have studied time evolution of the filling numbers in the system of two interacting QDs coupled with continuous-spectrum states in the presence of Coulomb interaction for a wide range of the system parameters. Different initial charge configurations were considered. The solution describing the system dynamics was analyzed under the assumption that the band and localized filling numbers for the electrons are uncoupled. This solution exactly takes all-order correlators for the localized electrons in the QDs into account.

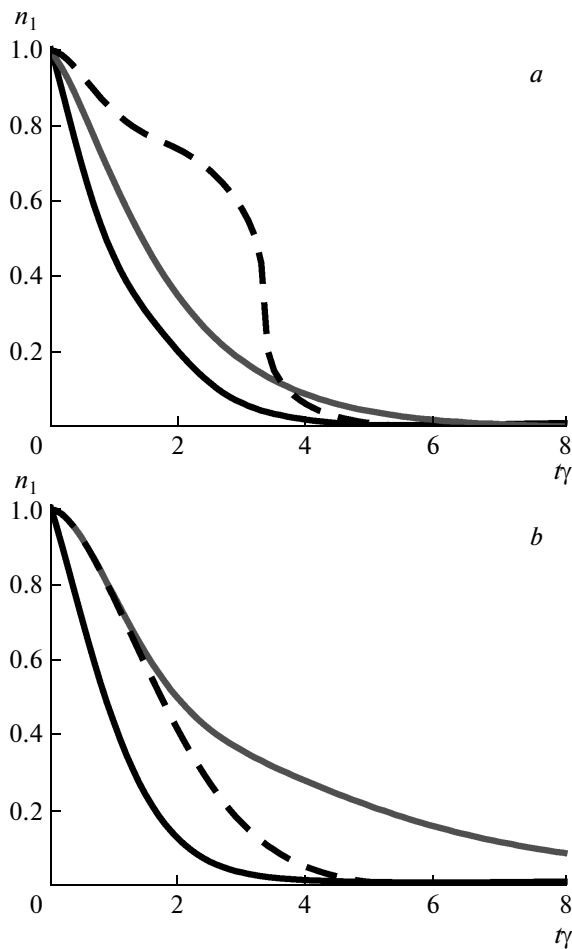


Fig. 6. Relaxation of the filling numbers $n_1(t)$ in the presence of Coulomb interaction in the case of resonant tunneling between the empty energy levels in the QDs. The black lines correspond to the exact solution, the black dashed lines correspond to the mean-field approximation. The grey lines demonstrate relaxation of the localized charge in the absence of Coulomb interaction. *a)* $\xi/\gamma = 0$ and $(U_1 - U_2)/\gamma = 3$; *b)* $\xi/\gamma = 0$ and $(U_1 - U_2)/\gamma = 1$. The parameters $T/\gamma = 0.6$ and $\gamma = 1$ are the same for all figures

We found strongly different relaxation regimes in the system of coupled QDs depending on the ratios between the system parameters. An interesting manifestation of Coulomb correlations is the formation of a dip in the time evolution of the localized charge. Such reentrant charge behavior is not the result of simple quantum oscillations between the two energy levels.

We compared our results with the mean-field approximation. The mean-field approximation can in some cases give qualitatively similar peculiarities of the system behavior: several time ranges with considerably

different relaxation rates and dip formation. But the mean-field approximation results do not coincide with the exact solution in many regimes. Even if the mean-field approximation qualitatively correctly predicts the appearance of the dip, its shape and width strongly differ from those given by the exact solution.

We acknowledge the financial support from the RFBR and Leading Scientific School grants. This work was also supported by the Russian Federation Presidential Grant for Young Scientists MK2780.2013.2.

REFERENCES

1. C. P. Collier, E. W. Wong, M. Belohradsky, F. M. Raymo, J. F. Stoddart, P. J. Kuekes, R. S. Williams, and J. R. Heath, *Science* **285**, 391 (1999).
2. D. I. Gittins, D. Bethell, D. J. Schiffrin, and R. J. Nichols, *Nature* **408**, 67 (2000).
3. M. A. Kastner, *Rev. Mod. Phys.* **4**, 849 (1992).
4. R. Ashoori, *Nature* **379**, 413 (1996).
5. T. H. Oosterkamp, T. Fujisawa, W. G. van der Wiel, K. Ishibashi, R. V. Hijman, S. Tarucha, and L. P. Kouwenhoven, *Nature* **395**, 873 (1998).
6. R. H. Blick, D. van der Weide, R. J. Haug, and K. Eberl, *Phys. Rev. Lett.* **81**, 689 (1998).
7. C. A. Stafford and N. Wingreen, *Phys. Rev. Lett.* **76**, 1916 (1996).
8. B. L. Hazelzet, M. R. Wagewijs, T. H. Stoof, and Yu. V. Nazarov, *Phys. Rev. B* **63**, 165313 (2001).
9. E. Cota, R. Aguadado, and G. Platero, *Phys. Rev. Lett.* **94**, 107202 (2005).
10. F. R. Waugh, M. J. Berry, D. J. Mar, R. M. Westervelt, K. L. Campman, and A. C. Gossard, *Phys. Rev. Lett.* **75**, 705 (1995).
11. R. H. Blick, R. J. Haug, J. Weis, D. Pfannkuche, K. V. Klitzing, and K. Eberl, *Phys. Rev. B* **53**, 7899 (1996).
12. C. A. Stafford and S. Das Sarma, *Phys. Rev. Lett.* **72**, 3590 (1994).
13. K. A. Matveev, L. I. Glazman, and H. U. Baranger, *Phys. Rev. B* **54**, 5637 (1996).
14. A. N. Vamivakas, C.-Y. Lu, C. Matthiesen, Y. Zhao, S. Fält, A. Badolato, and M. Atatüre, *Nature Lett.* **467**, 297 (2010).

15. E. A. Stinaff, M. Scheibner, A. S. Bracker, I. V. Ponomarev, V. L. Korenev, M. E. Ware, M. F. Doty, T. L. Reinecke, and D. Gammon, *Science* **311**, 636 (2006).
16. J. M. Elzerman, K. M. Weiss, J. Miguel-Sanchez, and A. Imimoğlu, *Phys. Rev. Lett.* **107**, 017401 (2011).
17. K. Kikoin and Y. Avishai, *Phys. Rev. B* **65**, 115329 (2002).
18. J. Peng and G. Bester, *Phys. Rev. B* **82**, 235314 (2010).
19. G. Munoz-Matutano, M. Royo, J. I. Climente, J. Canet-Ferrer, D. Fuster, P. Alonso-González, I. Fernández-Martínez, J. Martínez-Pastor, Y. González, L. González, F. Briones, and B. Alén, *Phys. Rev. B* **84**, 041308(R) (2011).
20. S. J. Angus, A. J. Ferguson, A. S. Dzurak, and R. G. Clark, *Nano Lett.* **7**, 2051 (2007).
21. K. Grove-Rasmussen, H. Jorgensen, T. Hayashi, P. E. Lindelof, and T. Fujisawa, *Nano Lett.* **8**, 1055 (2008).
22. S. Moriyama, D. Tsuya, E. Watanabe, S. Uji, M. Shimizu, T. Mori, T. Yamaguchi, and K. Ishibashi, *Nano Lett.* **9**, 2891 (2009).
23. R. Landauer, *Science* **272**, 1914 (1996).
24. D. Loss and D. P. DiVincenzo, *Phys. Rev. A* **57**, 120 (1998).
25. S. E. Nigg and M. Büttiker, *Phys. Rev. Lett.* **102**, 236801 (2009).
26. M. Filippone, K. Le Hur, and C. Mora, *Phys. Rev. Lett.* **107**, 176601 (2011).
27. K. Y. Tan, K. W. Chan, M. Möttönen, A. Morello, C. Yang, J. van Donkelaar, A. Alves, J.-M. Pirkkalainen, D. N. Jamieson, R. G. Clark, and A. S. Dzurak, *Nano Lett.* **10**, 11 (2010).
28. L. C. L. Hollenberg, A. D. Greentree, A. G. Fowler, and C. J. Wellard, *Phys. Rev. B* **74**, 045311 (2006).
29. G. Feve, A. Mahé, J.-M. Berroir, T. Kontos, B. Plaais, D. C. Glattli, A. Cavanna, B. Etienne, and Y. Jin, *Science* **316**, 1169 (2007).
30. M. Lee, R. López, M.-S. Choi, T. Jonckheere, and T. Martin, *Phys. Rev. B* **83**, 201304(R) (2011).
31. F. Recker mann, J. Splettstoesser, and M. R. Wegewijs, *Phys. Rev. Lett.* **104**, 226803 (2010).
32. T. Hayashi, T. Fujisawa, H. Cheong, Y. H. Jeong, and Y. Hirayama, *Phys. Rev. Lett.* **91**, 226804 (2003).
33. S. A. Gurvitz and M. S. Marinov, *Phys. Rev. A* **40**, 2166 (1989).
34. S. A. Gurvitz and G. Kalbermann, *Phys. Rev. Lett.* **59**, 262 (1987).
35. L. D. Contreras-Pulido, J. Splettstoesser, M. Governale, J. König, and M. Büttiker, *Phys. Rev. B* **85**, 075301 (2012).
36. P. I. Arseyev, N. S. Maslova, and V. N. Mantsevich, *Pis'ma v Zh. Eksp. Teor. Fiz.* **95**, 521 (2012).
37. P. I. Arseyev, N. S. Maslova, and V. N. Mantsevich, *Europ. Phys. J. B* **85**(7), 249 (2012).
38. V. N. Mantsevich, N. S. Maslova, and P. I. Arseyev, *Sol. St. Comm.* **152**, 1545 (2012).
39. S. A. Gurvitz and Ya. S. Prager, *Phys. Rev. B* **53**, 15932 (1996).
40. S. A. Gurvitz, *Phys. Rev. B* **57**, 6602 (1998).
41. K. Kikoin and Y. Avishai, *Phys. Rev. Lett.* **86**, 2090 (2001).
42. P. W. Anderson, *Phys. Rev.* **124**, 41 (1961).
43. V. N. Mantsevich and N. S. Maslova, *Sol. St. Comm.* **150**, 2072 (2010).